2. Interfacial and Dimensional Constraints

While materials such as ceramics, metals, oxides, exhibit size limitations ('quantum well effects') only noticeable below 10 nm, it was found that in complex organic systems such as polymers, interfacial effects could be noticeable over distances of tens of nanometers.[11] Mean-field theories applied to interfacially constrained and size-limited polymer systems failed to describe the rather unexpected *mesoscale behavior* observed experimentally. The extension of the interfacial boundary far into the bulk was unexpected because many amorphous polymer systems were in the past theoretically treated as van der Waals liquids with an interaction length on the order of the radius of gyration, i.e., the effective molecular size. As in the vicinity of solid interfaces, the radius of gyration is compressed, it was reasonable to assume that interfacial effects are confined within this so-called *pinning regime* (~ 1 nm). Inside the pinning regime, it is commonly accepted that the material is structurally altered and exotic properties (for instance, quantum-well effects) are expected. Outside the pinning regime, complex materials, such as polymers, were expected to behave bulk-like.

Already our pioneering experiments, as early as 1994, have shown that such scaling theories fail. They do not explain observed unique mesoscale properties in thin films of thickness of tens of nanometers,[12] because they do not consider long-range coupling (see for instance Fig. 1-5), cooperative phenomena as discussed above, or material heterogeneities (discussed below). Also with mean-field approaches, it is generally assumed systems to be thermally equilibrated. We have tackled over the years a variety of aspects that involved interfacial constraints. From a fundamental perspective, two have been of particular interest to us, involving ultrathin polymer systems: (i) the glass transition, and (ii) low dimensional flow. Another aspect of interest has been interfacial constraints and boundary layer formations in simple liquids. The following subsections illuminate these three topics in greater detail and provide some insight into our research involvements.

2.1 Low Dimensional Flow – Wetting and Dewetting of Polymer Films

The process of wetting of surfaces by liquids within the mesoscale is very complex and of interest to us for many reasons. In ultrathin film lubrication, for instance, the wettability of the liquid is of enormous importance, as it affects the hydrodynamic slip length (an extrapolated length for non-zero velocities at the wall). Wetting phenomena are important for flow in micro or submicrometer conduits (e.g., membrane systems, and microfluidic flow systems). The spreading of “completely-wetting” polymer liquids on solid surfaces has revealed unexpected spatial and temporal features when examined at the molecular level. The spreading profile is typically characterized by the appearance of a precursor film of monomolecular thickness extending over macroscopic distances, and in many cases, a terracing (also on the order of molecular dimensions) of the fluid remaining in the reservoir (Heslot et al. (1989))**.** These spatial features have been shown to be consistent with a Poiseuille-like flow in which the disjoining pressure gradients with film thickness drive the spreading process (Karis et al. (1999)). The temporal evolution of the spreading profile in this film thickness regime is, however, found to universally scale as $t^{1/2}$ even at short times (Heslot et al. (1989)). That the spreading dynamics are reflective of a diffusive transport mechanism, and not of a pressure driven “liquid” flow, suggests that interfacial confinement substantially alters the mobility of molecularly-thin polymer fluids.

Confined flow properties have been addressed in our research from monolayer lubrication,[13] to flow and wetting/dewetting characteristics in homopolymer, graft copolymers and polymer multiphase systems[12,14,15]. The wetting behavior of polymer thin films has received a great amount of attention, because of its importance in practical applications. The effect of an attractive solid interface on the polymer mobility was investigated and found to decrease diffusion significantly.[14,15] In a number of systems, we observed that the wettability of the surface is determined by the ability of the polymer melt to penetrate into the restricted polymer substrate such as a densely adsorbed polymer brush, a self-assembled surface of diblock copolymer with chemically dissimilar blocks, or a cross-linked surface.[12,14,15] Even if the melt and the substrate

are of identical chemical structure, entropy considerations limit the penetration of the melt chains into the substrate, leading to partial wetting. This phenomenon is referred to as “wetting autophobicity”. The physical origins of wetting autophobicity in polymeric systems can be attributed to limitations on the molecular configurations of the restricted polymer substrates.

2.1.1 Interfacial Excess Energy Induced Dewetting

In our research involving binary polymer systems, we addressed the role of the molecular architecture of the substrate on the wetting characteristic of polymer melts.[12,14] A series of model graft copolymers of constant molecular weight but different number of grafts was used to investigate the dewetting behavior with chemically identical homopolymer films.[14] The graft copolymers consisted of a deuterated poly(ethyl acrylate) (dPEA) backbone with one, three, or five pendant chains of monodisperse polystyrene (PS) attached randomly along its length (dPEA-g-xPS, *x*)1, 3, 5). The graft copolymers are ordered on silicon substrates with the lower-energy dPEA back-bone at the vacuum interface. The equilibrium structures are shown in Figure 2-1(a) determined by SIMS. The dewetting behavior of dPEA and PS homopolymer films on the ordered graft copolymer substrates was studied by scanning probe microscopy (SPM) techniques, Fig. 2-1(b) and (c), from which interfacial tensions were deduced.

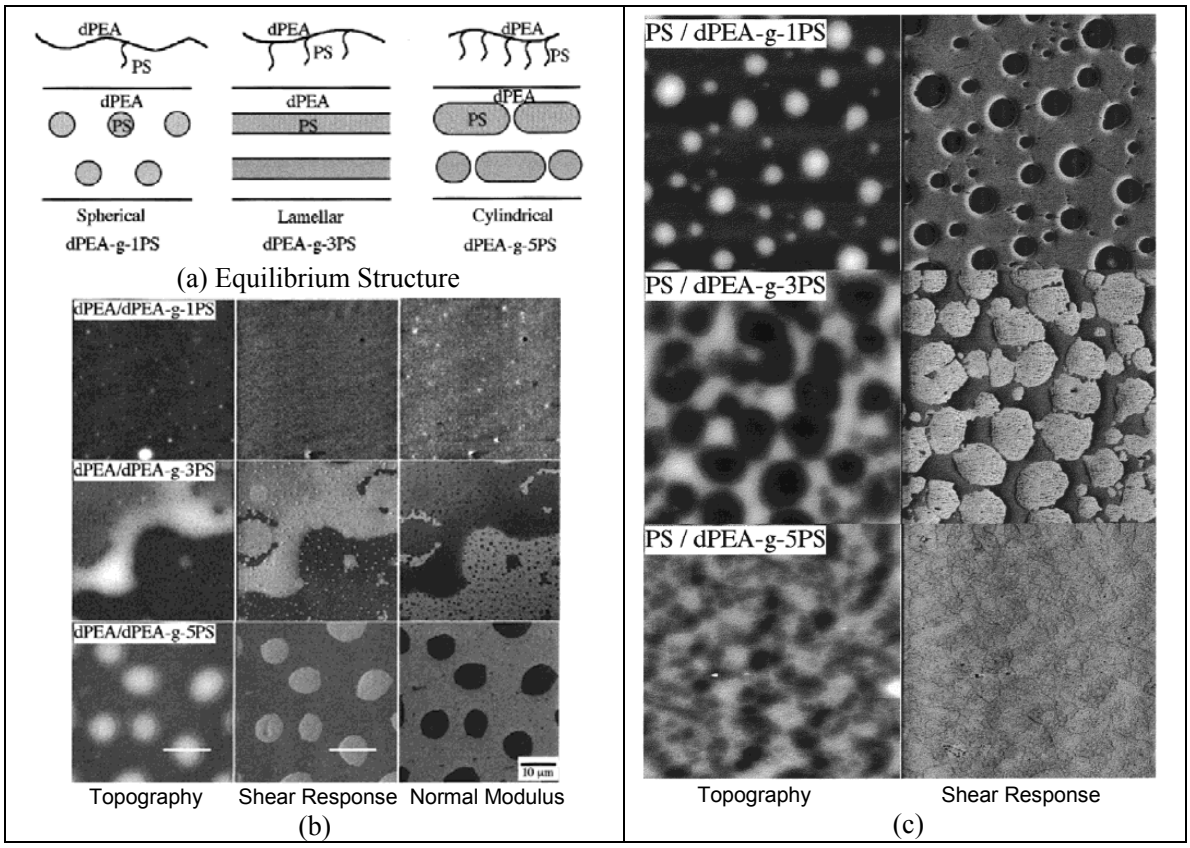

Fig. 2-1: (*a*) Equilibrium structure of dPEA-g-xPS (x = 1,3,5). (*b*) SPM measurements of dPEA-g-3PS and dPEA-g-5PS graft copolymers covered by dPEA homopolymer. (*c*) SPM measurements of the dPEA-g-xPS graft copolymers covered by PS homopolymer. All systems have been annealed at 450 K for 24 h.[14]

The study revealed that for the lower viscosity homopolymer dPEA, the excess energy associated with the interface between dPEA-PS graft copolymer and the homopolymer can destabilize the film and induce dewetting. For the PS homopolymer, because the viscosity is greater than that of the substrate, the dewetting behavior on the dPEA-g-xPS substrate depends

on the substrate viscosity. The order of the dewetting velocity of the PS homopolymer on the graft copolymer was determined as: dPEA-g-1PS > dPEA-g-3PS > dPEA-g-5PS.

2.1.2 Finite Size Systems – Ultrathin Films

Subtle relative differences in the surface energies or viscous properties can significantly alter the flow behavior, as shown above, - as can interfacial modifications of the material phase. This last aspect becomes apparent in our dewetting studies on binary films with polystyrene (PS) covering thin films of polyethylene-co-propylene (PEP) that were spun onto silicon substrates (high interaction surface).[12,16] The dewetting kinetics in Figure 2-2 were determined from a time-series of SPM topography images, and reveal a critical PEP film thickness, δ_{CRIT}, of ~ 100 nm, below which the dewetting velocity (v_d) decreases with decreasing film thickness, and above which, v_d remains constant. Independent friction force microscopy experiments (a method to determine material phase differences,[5,9] and probe local rheological properties) on PEP alone, Fig. 2-2, attribute the changes in the dewetting process on phase changes in the PEP matrix. While today such observations are not astonishing, they were quite surprising in 1995, when it was common practice to assume that after annealing a film thicker than a few nanometers behaves bulk-like. The dewetting kinetics and friction forces both suggest the presence of a rheologically modified PEP boundary layer adjacent to the silicon surface. For $\delta_{PEP} < \delta_{CRIT}$, the decreasing friction represents an increase in the PEP modulus. This translates to an increasing *glass-like* behavior, or loss of mobility, as the silicon interface is approached through the PEP phase. It is this loss of PEP mobility that is responsible for decreasing the dewetting velocity.

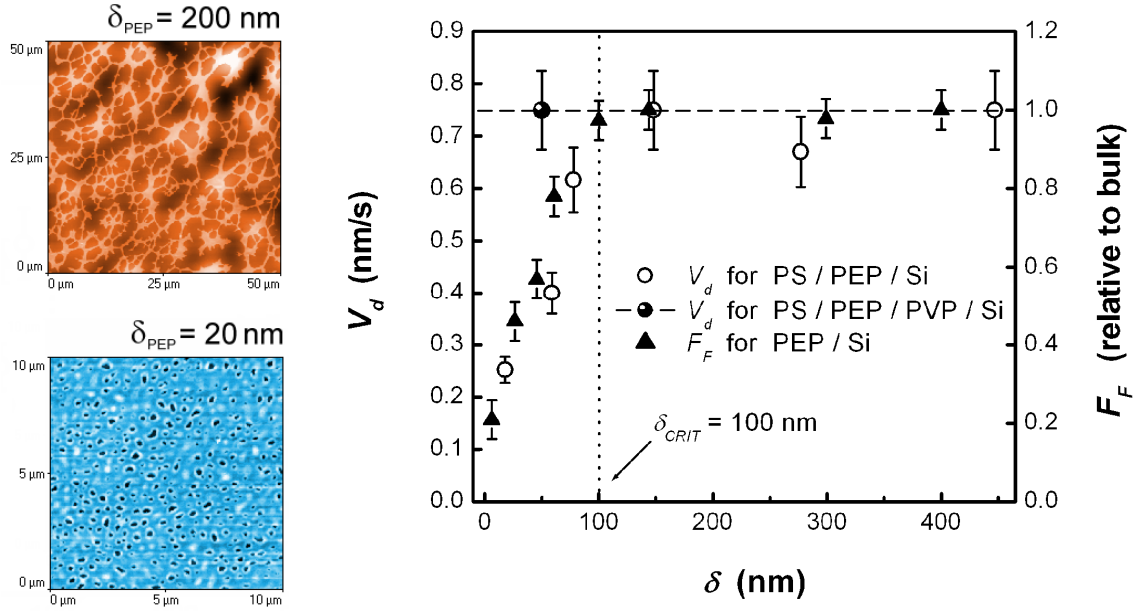

Fig. 2-2: (*Left*) PS dewetting of PEP. PS film thickness 10 nm. (*Right*) Dewetting velocity (v_d) and friction (F_F) measurements on PS/PEP systems reveal a 100 nm interfacial boundary layer.[12,16]

To identify the source of this rheological gradient, the PEP-silicon interactions were effectively masked by first spin casting a low interaction foundation layer of poly(vinyl pyridine) (PVP) on the silicon. The dewetting velocity of the PS/PEP/PVP layered film system, represented in Figure 2-2 by the filled circle and the dashed horizontal line, remained constant, even at PEP film thicknesses below δ_{CRIT}. This finding unveils the high interfacial interactions between PEP and silicon as responsible for the apparent PEP vitrification inside the interfacial boundary.

Our nanoscopic friction (F_F vs. F_N) experiments on silicon supported PEP films (R_G = 24 nm) offered further insight to the source of these *far-field* molecular constraints beyond the pinning

regime.[16] A transition in the friction coefficient at a critical load (*P*) is seen in Figure 2-3(*Left*). The higher friction coefficient below *P* portrays a dissipative behavior consistent with viscous plowing through an entangled PEP melt. We found that the transition load, *P*, fulfilled the criteria of a maximum load because no further strain occured at higher load.[16] This allowed us to determine the load independent work of adhesion (per unit contact area), via

$$\gamma_D = \frac{1}{3\pi R}\lim_{P_{\max}\to 0} F_{adh}(P_{\max}) = \frac{F_D}{3\pi R}, \qquad (2.1)$$

which yielded for γ_D a value of 53 dyn/cm. Plotting the transition load versus the instability adhesion force, F_{adh}, a Dupré adhesion force F_D of 5 nN could be interpolated at zero load, Fig. 2-3 (*right*). We found that these values were in excellent agreement with the literature.

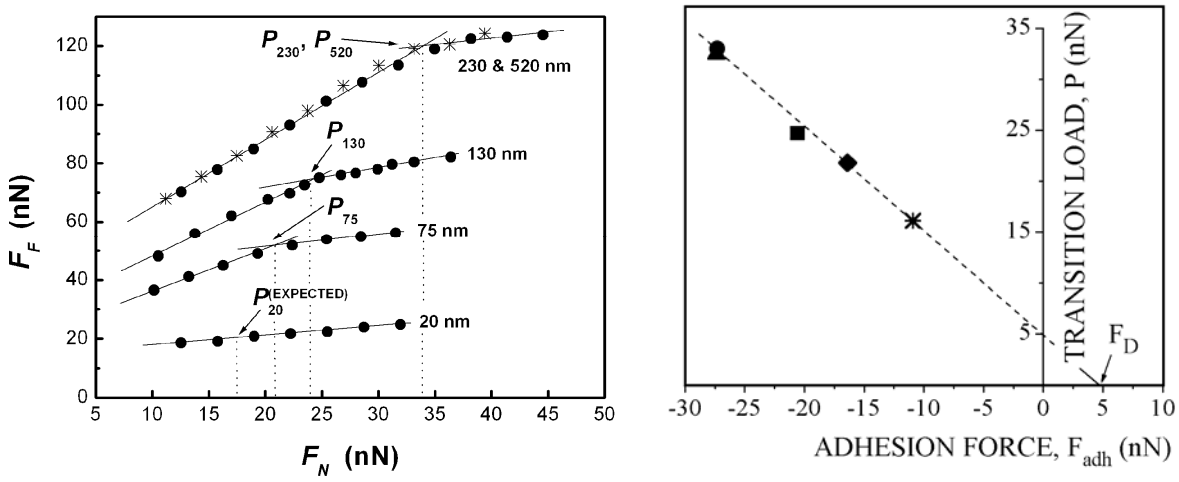

Fig. 2-3: (*Left*) SPM friction experiments on PEP films reveal a critical load (*P*) marking a transition from viscous shearing to chain sliding. F_N is the sum of the adhesion and applied load. (*Right*) Functional relationship between the adhesion force and the transition load, *P*, for 75-520 nm film thickness. F_D corresponds to the Dupré adhesion. [16]

Our study exposed a two phase low dimensional flow regime comprised of a *sublayer* and an *intermediate regime*. The mobility constraints are ascribed to the strain imposed during spin casting, paired with interfacial interactions in the sublayer and anisotropic diffusion in the intermediate regime. At loads exceeding *P*, the reduced friction coefficient represents a chain slipping phenomenon similar to a shear banding behavior. Thus, the critical load may be conceptualized as an effective activation barrier for disentanglement. The boundary layer thickness and information about to the conformational structure within the boundary are elucidated from the film thickness dependence of *P*:

(i) The absence of the disentanglement transition (*P*) in the 20 nm films and the ubiquitous low friction, chain slipping suggests that the PEP molecules are highly disentangled within a *sublayer* immediately adjacent to the substrate.

(ii) In the 75-230 nm films, the disentanglement transition (*P*) increases linearly with film thickness until the bulk *P* is reached. The sub-bulk *P* values indicate an *intermediate regime* of partial disentanglement, the extent of which diminishes with increasing film thickness until the bulk entanglement density is recovered. This far-field disentanglement (~ 10 R_G from the substrate) is attributed to the strain imposed during spin casting. The preservation of the disentangled structure in the melt reflects an anisotropic diffusion process where partially disentangled chain ends diffuse into the more porous structure of sublayer.

(iii) Finally, for films thicker than 230 nm, the polymer behaves like the bulk elastomer and loses any memory of the underlying silicon.

2.2 Glass Transition in Ultrathin Films

With the discovery of far-field interfacial effects in complex polymeric systems, we intensified our efforts in studying the impact of interfacial constraints in ultrathin films on one of the technologically most important but apparently nonspecific polymer property, the glass transition temperature T_g. In experiments, the glass transition is typically referred to as calorimetric glass transition, as the notion exists that T_g is not an actual material property (or material distinctive critical quantity), but to some degree a manifestation of the impatience of the experimentalist. This perception originated from the existing gap between theory and experiments, which until recently was lacking any correspondence between theoretical glass transition models, such as the mode-coupling theory and calorimetric glass transition experiments.[10]

Our first step was to devise a technique with which to determine the glass transition of thin film systems. Motivated by our success using SPM friction as a phase distinctive tool (see above), we developed a SPM approach based on lateral forces, referred to as shear modulation force microscopy (SM-FM).[17] SM-FM has turned out to be an excellent tool to determine any sort of transitions and relaxations at polymer surfaces. It is a non-scanning method.

Briefly: A nanometer sharp scanning force microscopy (SFM) cantilever tip is brought into contact with the sample surface as illustrated in Figure 2-4(*left*). While a constant load is applied, the probing tip is laterally modulated with a "no-slip" nanometer amplitude, ΔX_{IN}. The modulation response, ΔX_{OUT}, is analyzed after each temperature step using a two-channel lock-in amplifier, comparing the response signal to the input signal. The modulation response is a measure of the contact stiffness. Thermally activated transitions in the material, such as the glass transition, T_g, are determined from the "kink" in the response curve, as shown in the same graph, and in Figure 2-4(*right*), as function of the molecular weight of the polymer [18]. With a computer acquisition setup great care is taken to stay close to steady state after each temperature step (~ 0.1 to 0.5 °C).

Conceptually, SM-FM is a nanoscopic analogue to dynamic mechanical analysis (DMA), however, because of its small probing volume, SM-FM is probing very close to the material's unperturbed state. This last statement is one of the most important findings of our research involving T_g. In conjunction with the IFA analysis (c.f. sec. 1.2), we established T_g to be a truly distinctive critical thermal property of the material. As discussed above, Fig. 1-5(*Right*), it turned out that T_g is well described by theoretical transition temperatures, such as the mode coupling temperature.

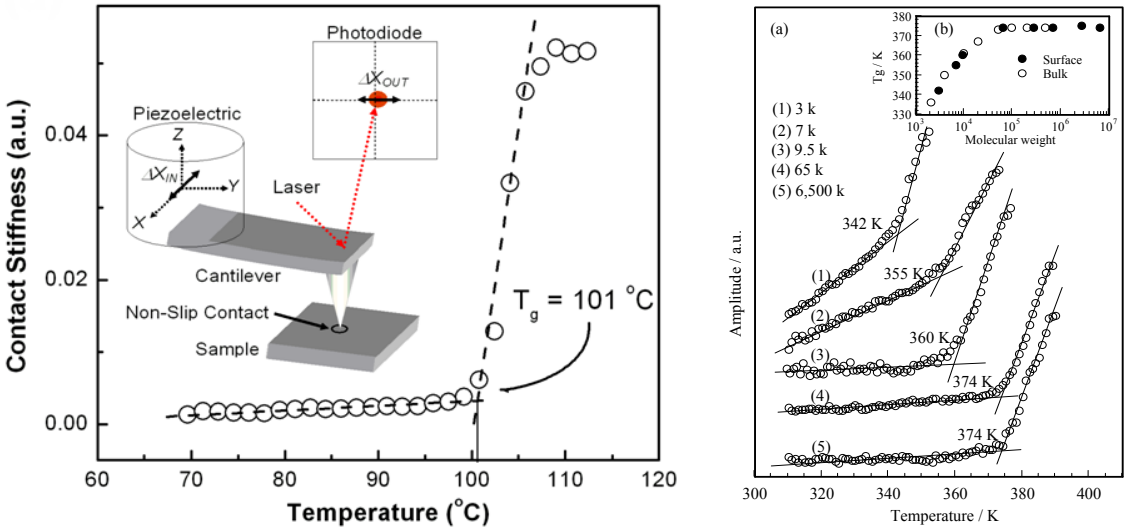

Fig. 2-4: (*Left*) SM-FM working principle. Illustrated on atactic monodisperse polystyrene (M_w 90k).[17] (*Right*). (a) SM-FM molecular weight series of polystyrene. (b) SM-FM Tg values correspond well to bulk values determined by differential scanning calorimetry.[18]

With the successful development of an analysis tool sensitive to near-surface thermal transitions in thin films, we were ready to study the effect of substrate confinement on the glass transition. Although, we recognized the importance of impurities and monodispersity (low molecular weight polymer have a high preponderance at the free surface), it turned out that SM-FM experiments are by far less delicate to perform as originally assumed. We recognized that several factors are intricately responsible for the departure of T_g in ultrathin films from the bulk value;[7] (i) the proximity of a free surface, (ii) substrate interactions, and (iii) process-induced anisotropy. Here, I briefly summarize our findings on the effects of spin casting on the interfacial T_g profile of amorphous polymer films, along with the use of chemical crosslinking as a mobility control.

SM-FM T_g measurements on PS films (M_w =12k) are presented in Figure 2-5 (*Left*). For film thicknesses, δ > ~100 nm, the T_g values correspond to the bulk T_g of 95°C.[7] As in the friction study presented above, a two phase boundary layer is encountered within ~100 nm of the substrate: (a) T_g values are depressed relative to the bulk in a *sublayer* with a thickness on the order of R_G, i.e. one order of magnitude beyond the persistence length; and (b) T_g values exceed the those of the bulk in the *intermediate regime*. Thus, the origin for the non-monotonic $T_g(\delta)$ relationship is due to shear induced structuring imposed by the film processing condition (spin coating) followed by interdiffusion.[7]

While the dominant change in T_g, i.e., the decrease is widely acknowledged for ultrathin polymer films, the less pronounced increase has rarely been observed by other groups, due to instrumental sensitivity limitations. We, on the other hand, observed a non-monotonic $T_g(\delta)$ profile for various spin coated polymer thin films. I will show later (subsection 4.3), the significance of this profile for engineering applications. In the next two paragraphs, our research in this field, involving $T_g(\delta)$ profile modification by imposing additional constraints will be illustrated.

One way of altering interfacial constraints is by changing the molecular weight (M_w). Increased M_w in spin cast films had the effect of shifting the glass transition maximum in the $T_g(\delta)$ profiles further away from the substrate, as shown in Fig. 2-5(*Right*).[7] Consequently, the bulk T_g is recovered for thicker films. The influence of M_w on the internal structure of the boundary layer appears more pronounced on the sublayer thickness than on the far-field boundary of the intermediate regime. This suggests that the overall boundary thickness depends more strongly on the spin casting shear stresses than on molecular dimensions.

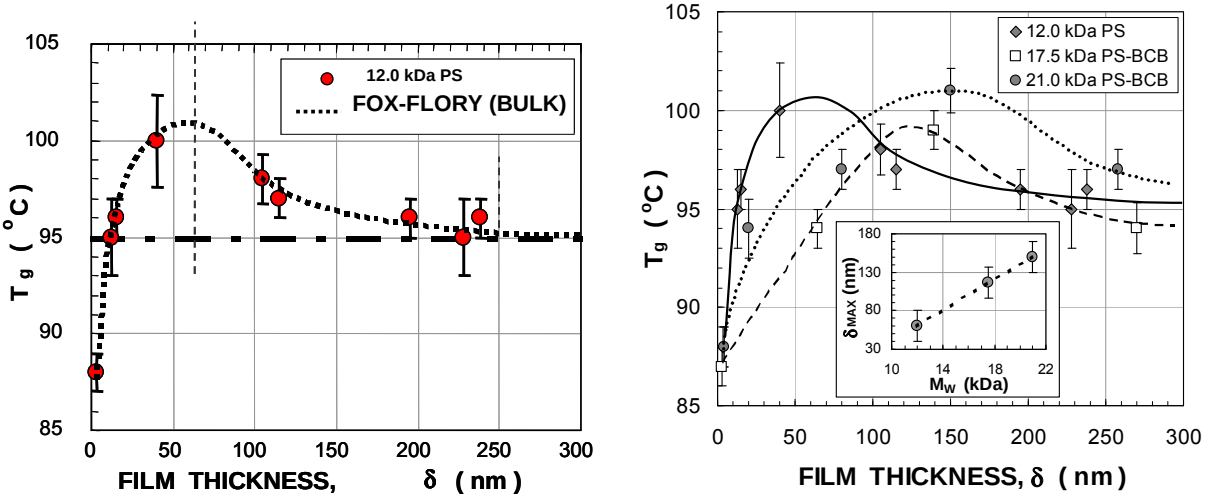

Figure 2-5: (*Left*) (top) Film thickness, δ, dependence of T_g for PS films (Mw = 12k) compared to the bulk T_g from Fox-Flory theory. (*Right*) $T_g(\delta)$ profiles as function of the molecular weight. *Inset*: Linear relationship between the maximum thickness δ_{max} (defined by the maximum T_g value) in each profile with the corresponding molecular weight M_W.[7]

Furthermore, we imposed internal constraints by crosslinking.[7] Polystyrene-benzocyclobutane (PS-BCB) films exhibited qualitative similar and vertically shifted $T_g(\delta)$ profiles before and after crosslinking, as illustrated in Fig. 2-6. Thereby, crosslinking yielded an overall T_g increase (7±3 °C in this case); however, in contrast to the M_W dependence discussed above, no horizontal spatial shifts occurred.

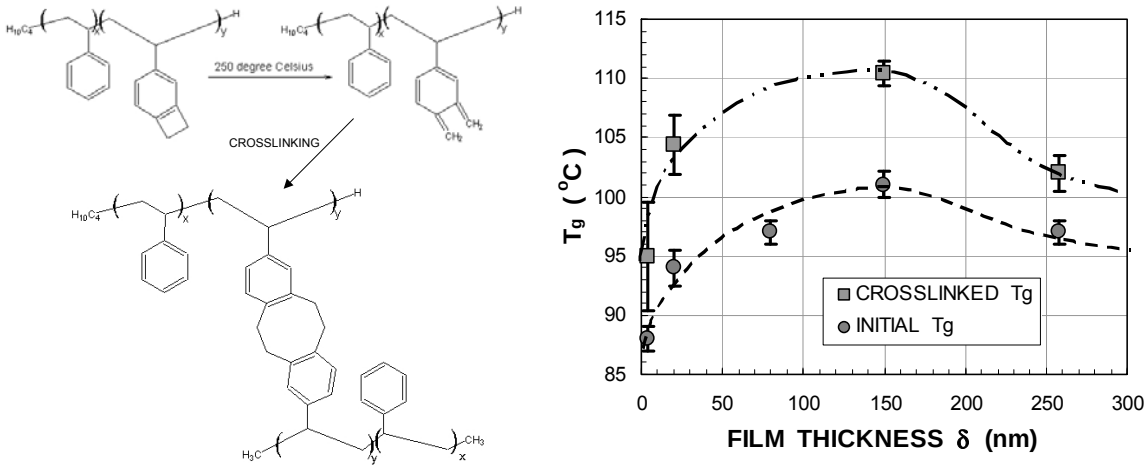

Fig. 2-6: (*Left*) PS-BCB crosslinking mechanism. (*Right*) $T_g(\delta)$ profile for PS-BCB thin films (21kDa PS-4.8 mol% BCB) before and after crosslinking (crosslinked at 250°C under N_2 for 1 hr).[7]

Thus, our research has not only provided us with fundamental insight into constraint-modified transition properties on the sub-100 nanometer scale, but also with control parameters that allow us to adjust transition profiles accordingly to desired material behavior, an aspect, that is discussed in greater detail in subsection 4.3. We also learned from the two imposed constraints that the impact of mobility constraints on the structure within the boundary layer depends on the sequence of the film preparation process.[7] Something that is crucially important and often neglected in theoretical models.

2.3 Interfacial Dimensional Constraints - Entropic Cooling in Simple Liquids

At this point of section 2, we switch from condensed solid polymeric and interactive systems to “simple”, low interactive condensed fluid systems. Our interest is in determining how dimensional constraints at 2D interfaces are impacting the phase behaviour of liquids in the boundary regime. This aspect of our research is illustrated with our nanoscopic study of two hydrocarbon fluids of significant different molecular shape.

We were curious about the effect of an ultra-smooth planar surface on self-induced local “structuring”, or more to the point, *entropic cooling*, involving the two hydrocarbon liquids n-hexadecane and octamethylcyclotetrasiloxane (OMCTS). These two material systems sparked our interest as they had been repeatedly studied by surface forces apparatus (SFA), revealing a layering of the liquid molecules under compression involving two smooth interfaces. Curiously, some molecular dynamic simulations claimed to confirm this behavior with only one interface. Our experiment[2] involved ultrasharp probing SFM tips (with ~1 - 5 nm radius at the tip apex), which were sinusoidally shear-modulated and lowered within the liquids to the surface with nm/s speeds. Such a shear modulation analysis, as illustrated in Figure 2-7(*Top*), is very close to equilibrium probing. It combines normal tip-sample interaction force measurements with shear amplitude response information. Differences in the onset of change in the two mentioned signals during an approach provide a direct measure of the boundary layer thickness.

Figure 2-7(*Right*) presents the results of the two liquid hydrocarbon liquids, and water that served as discriminator for our instrumental accuracy. The experiment revealed only for the linear n-hexadecane an entropically cooled, interfacially layered fluid boundary of 2 nm thickness, while OMCTS, consisting of spherically shaped molecules, exhibited only an interfacial 'monolayer'.

Thus, while our results regarding n-hexadecane compared well with SFA experiments (i.e., half of the maximum layer thickness involving two surfaces), our OMCTS results were significantly smaller. The major difference between SFA and our SFM experiment is the lateral probing or confining dimension. While during SFM experiment the molecules can easily escape from underneath the tip, it is far more difficult for them to escape from between the micron-sized confining surface planes of SFA. In SFA liquid molecules are temporarily trapped that gives rise to density fluctuations, and thus, oscillatory solvation forces. In our SFM experiment, on the other hand, trapping effects are negligible.

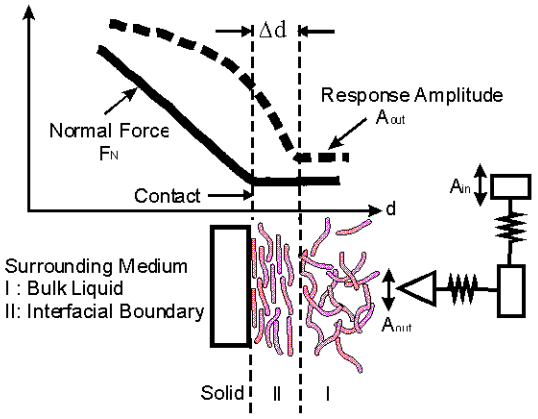

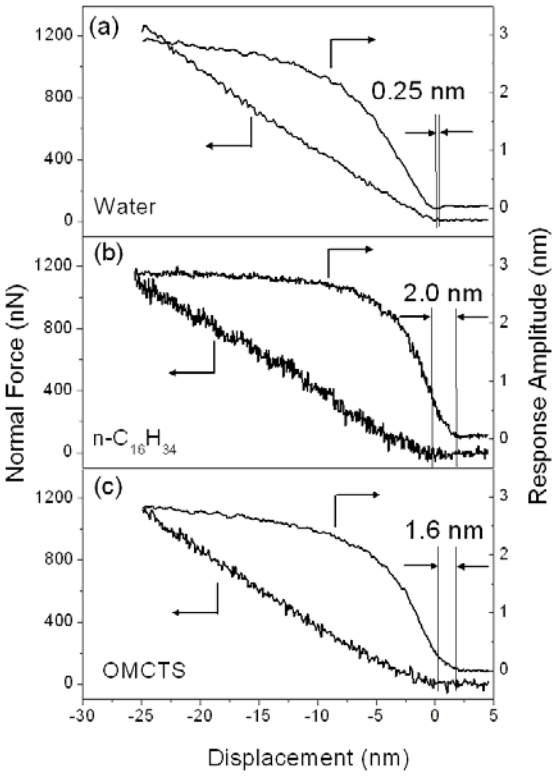

Fig. 2-7(*Top*): Illustration of the shear modulation SFM approach methodology that provides the boundary layer thickness Δd from the difference in the onset of change of the shear modulation response curve and contact force curve.
Fig. 2-7(*Right*): Shear modulated force displacement measurements towards silicon oxide surfaces with an approach velocity of 5 nm/s at 21 °C in (a) water, (b) n-hexadecane and (c) OMCTS. The measurements were obtained with stiff rectangular SFM cantilevers (37-55 N/m), to avoid any snap-in instabilities, and with a shear amplitude of 3 nm (RMS) at 5kHz modulation.[2]

Consequently, we concluded that n-hexadecane molecules due to their highly anisotropic shape experience an interfacial alignment over an interfacial boundary regime of 2 nm that is affecting the SFM shear response. OMTCS on the other hand because of its more isotropic spherical shape is only affected in the molecular pinning regime, i.e., only when the molecules are in direct contact with the solid surface. It is interesting to note that these ultrathin boundary layers have a significant impact on the lubricating shear properties (c.f. sec. 3.2). From a viscometric perspective one would assume hexadecane to be a less effective lubricant as its viscosity exceeds the one of OMCTS in average by about 30 %. Experiments, however, show hexadecane to be the better (the lower friction, and friction coefficient) lubricant of the two.[2] Although astonishing from a viscometric perspective, it is predictable from the here gained molecular insight into the boundary layer formation of a dimensionally constraint system. We will continue this discussion in the next section that deals with fundamentals in tribology.

6. References and Citations Therein

[1] D. B. Knorr, T. Gray, and R. M. Overney, *Cooperative and Submolecular Dissipation Mechanisms of Sliding Friction in Complex Organic Systems*, J. Chem. Phys. **129**, 074504 (2008).

[2] M. Y. He, A. S. Blum, G. Overney, and R. M. Overney, *Effect of interfacial liquid structuring on the coherence length in nanolubrication*, Physical Review Letters **88**, 154302 (2002).

[3] T. Gray, T. D. Kim, D. B. Knorr, J. D. Luo, A. K. Y. Jen, and R. M. Overney, *Mesoscale dynamics and cooperativity of networking dendronized nonlinear optical molecular glasses*, Nano Letters **8**, 754-9 (2008).

[4] D. B. Knorr, T. Gray, and R. M. Overney, *Intrinsic Friction Analysis - Novel Nanoscopic Access to Molecular Mobility in Constrained Organic Systems*, Ultramicroscopy **in press** (2008).

[5] R. M. Overney, E. Meyer, J. Frommer, D. Brodbeck, R. Luthi, L. Howald, H. J. Guntherodt, M. Fujihira, H. Takano, and Y. Gotoh, *Friction Measurements on Phase-Separated Thin-Films with a Modified Atomic Force Microscope*, Nature **359**, 133-5 (1992).

[6] T. Gray, R. M. Overney, M. Haller, J. Luo, and A. K. Y. Jen, *Low temperature relaxations and effects on poling efficiencies of dendronized nonlinear optical side-chain polymers*, Applied Physics Letters **86** (2005).

[7] S. Sills, R. M. Overney, W. Chau, V. Y. Lee, R. D. Miller, and J. Frommer, *Interfacial glass transition profiles in ultrathin, spin cast polymer films*, Journal of Chemical Physics **120**, 5334-8 (2004).

[8] S. Sills, T. Gray, and R. M. Overney, *Molecular dissipation phenomena of nanoscopic friction in the heterogeneous relaxation regime of a glass former*, Journal of Chemical Physics **123** (2005).

[9] R. Overney and E. Meyer, *Tribological Investigations Using Friction Force Microscopy*, Mat. Res. Soc. Bulletin **18**, 26-34 (1993).

[10] T. Gray, J. Killgore, J. D. Luo, A. K. Y. Jen, and R. M. Overney, *Molecular mobility and transitions in complex organic systems studied by shear force microscopy*, Nanotechnology **18** (2007).

[11] R.M. Overney and S. E. Sills, in *Interfacial Properties on the Submicron Scale*, edited by J. Frommer and R. M. Overney (Oxford Univ. Press, New York, 2001), p. 2-23.

[12] R. M. Overney, D. P. Leta, L. J. Fetters, Y. Liu, M. H. Rafailovich, and J. Sokolov, *Dewetting dynamics and nucleation of polymers observed by elastic and friction force microscopy*, Journal of Vacuum Science & Technology B **14**, 1276-9 (1996).

[13] R. M. Overney, G. Tindall, and J. Frommer, in *Handbook of Nanotechnology*, edited by B. Bhushan (1439-1453, Heidelberg, 2007).

[14] S. R. Ge, L. T. Guo, M. H. Rafailovich, J. Sokolov, R. M. Overney, C. Buenviaje, D. G. Peiffer, and S. A. Schwarz, *Wetting behavior of graft copolymer substrate with chemically identical homopolymer films*, Langmuir **17**, 1687-92 (2001).

[15] A. Karim, T. M. Slawecki, S. K. Kumar, J. F. Douglas, S. K. Satija, C. C. Han, T. P. Russell, Y. Liu, R. Overney, O. Sokolov, and M. H. Rafailovich, *Phase-separation-induced surface patterns in thin polymer blend films*, Macromolecules **31**, 857-62 (1998).

[16] C. Buenviaje, S. R. Ge, M. Rafailovich, J. Sokolov, J. M. Drake, and R. M. Overney, *Confined flow in polymer films at interfaces*, Langmuir **15**, 6446-50 (1999).

[17] R. M. Overney, C. Buenviaje, R. Luginbuhl, and F. Dinelli, *Glass and structural transitions measured at polymer surfaces on the nanoscale*, Journal of Thermal Analysis and Calorimetry **59**, 205-25 (2000).

[18] S. Ge, Y. Pu, W. Zhang, M. Rafailovich, J. Sokolov, C. Buenviaje, R. Buckmaster, and R. M. Overney, *Shear modulation force microscopy study of near surface glass transition temperatures*, Physical Review Letters **85**, 2340-3 (2000).

[19] E. Meyer, R. Overney, R. Luthi, D. Brodbeck, L. Howald, J. Frommer, H. J. Guntherodt, O. Wolter, M. Fujihira, H. Takano, and Y. Gotoh, *Friction Force Microscopy of Mixed Langmuir-Blodgett-Films*, Thin Solid Films **220**, 132-7 (1992).

[20] E. Meyer, R. Overney, D. Brodbeck, L. Howald, R. Luthi, J. Frommer, and H. J. Guntherodt, *Friction and Wear of Langmuir-Blodgett-Films Observed by Friction Force Microscopy*, Physical Review Letters **69**, 1777-80 (1992).

[21] L. Howald, R. Luthi, E. Meyer, G. Gerth, H. G. Haefke, R. Overney, and H. J. Guntherodt, *Friction Force Microscopy on Clean Surfaces of NaCL, NaF, and AgBr*, Journal of Vacuum Science & Technology B **12**, 2227-30 (1994).

[22] R. M. Overney, T. Bonner, E. Meyer, M. Reutschi, R. Luthi, L. Howald, J. Frommer, H. J. Guntherodt, M. Fujihara, and H. Takano, *Elasticity, Wear, and Friction Properties of Thin Organic Films Observed with Atomic-Force Microscopy*, Journal of Vacuum Science & Technology B **12**, 1973-6 (1994).

[23] R. M. Overney, H. Takano, M. Fujihira, W. Paulus, and H. Ringsdorf, *Anisotropy in Friction and Molecular Stick-Slip Motion*, Physical Review Letters **72**, 3546-9 (1994).
[24] R. M. Overney, H. Takano, and M. Fujihira, *Elastic Compliances Measured by Atomic-Force Microscopy*, Europhysics Letters **26**, 443-7 (1994).
[25] R. M. Overney, H. Takano, M. Fujihira, E. Meyer, and H. J. Guntherodt, *Wear, Friction and Sliding Speed Correlations on Langmuir-Blodgett-Films Observed by Atomic-Force Microscopy*, Thin Solid Films **240**, 105-9 (1994).
[26] F. Dinelli, C. Buenviaje, and R. M. Overney, *Glass transitions of thin polymeric films: Speed and load dependence in lateral force microscopy*, Journal of Chemical Physics **113**, 2043-8 (2000).
[27] C. Buenviaje, F. Dinelli, and R. M. Overney, *Investigations of heterogeneous ultrathin blends using lateral force microscopy*, Macromolecular Symposia **167**, 201-12 (2001).
[28] S. Sills and R. M. Overney, *Creeping friction dynamics and molecular dissipation mechanisms in glassy polymers*, Physical Review Letters **91**, 095501 (2003).
[29] S. Sills, H. Fong, C. Buenviaje, M. Sarikaya, and R. M. Overney, *Thermal transition measurements of polymer thin films by modulated nanoindentation*, Journal of Applied Physics **98** (2005).
[30] S. Sills, T. Gray, J. Frommer, and R. M. Overney, in *Applications of Scanned Probe Microscopy to Polymers*, 2005), Vol. 897, p. 98-111.
[31] S. Sills, R. M. Overney, B. Gotsmann, and J. Frommer, *Strain shielding and confined plasticity in thin polymer films: Impacts on thermomechanical data storage*, Tribology Letters **19**, 9-15 (2005).
[32] J. P. Killgore and R. M. Overney, *Interfacial mobility and bonding strength in nanocomposite thin film membranes*, Langmuir **24**, 3446-51 (2008).
[33] R. M. Overney, D. P. Leta, C. F. Pictroski, M. H. Rafailovich, Y. Liu, J. Quinn, J. Sokolov, A. Eisenberg, and G. Overney, *Compliance measurements of confined polystyrene solutions by atomic force microscopy*, Physical Review Letters **76**, 1272-5 (1996).
[34] M. Y. He, A. S. Blum, D. E. Aston, C. Buenviaje, R. M. Overney, and R. Luginbuhl, *Critical phenomena of water bridges in nanoasperity contacts*, Journal of Chemical Physics **114**, 1355-60 (2001).
[35] S. Sills, K. Vorvolakos, M.K. Chaudhury, and R. M. Overney, in *Friction and Wear on the Atomic Scale*, edited by E. Gnecco and E. Meyer (Springer Verlag, Heidelberg, 2007), p. 659-76.
[36] E. Meyer, L. Howald, R. M. Overney, H. Heinzelmann, J. Frommer, H. J. Guntherodt, T. Wagner, H. Schier, and S. Roth, *Molecular-Resolution Images of Langmuir-Blodgett-Films Using Atomic Force Microscopy*, Nature **349**, 398-400 (1991).
[37] R. Luthi, R. M. Overney, E. Meyer, L. Howald, D. Brodbeck, and H. J. Guntherodt, *Measurements on Langmuir-Blodgett-Films by Friction Force Microscopy*, Helvetica Physica Acta **65**, 866-7 (1992).
[38] F. Schabert, A. Hefti, K. Goldie, A. Stemmer, A. Engel, E. Meyer, R. Overney, and H. J. Guntherodt, *Ambient-Pressure Scanning Probe Microscopy of 2d Regular Protein Arrays*, Ultramicroscopy **42**, 1118-24 (1992).
[39] J. Frommer, R. Luthi, E. Meyer, D. Anselmetti, M. Dreier, R. Overney, H. J. Guntherodt, and M. Fujihira, *Adsorption at Domain Edges*, Nature **364**, 198- (1993).
[40] R. M. Overney, E. Meyer, J. Frommer, H. J. Guntherodt, M. Fujihira, H. Takano, and Y. Gotoh, *Force Microscopy Study of Friction and Elastic Compliance of Phase-Separated Organic Thin-Films*, Langmuir **10**, 1281-6 (1994).
[41] R. M. Overney, manuscript in preparation.
[42] T. Gray, C. Buenviaje, R. M. Overney, S. A. Jenekhe, L. X. Zheng, and A. K. Y. Jen, *Nanorheological approach for characterization of electroluminescent polymer thin films*, Applied Physics Letters **83**, 2563-5 (2003).
[43] T. D. Kim, J. W. Kang, J. D. Luo, S. H. Jang, J. W. Ka, N. Tucker, J. B. Benedict, L. R. Dalton, T. Gray, R. M. Overney, D. H. Park, W. N. Herman, and A. K. Y. Jen, *Ultralarge and thermally stable electro-optic activities from supramolecular self-assembled molecular glasses*, Journal of the American Chemical Society **129**, 488-9 (2007).
[44] J. H. Wei, M. Y. He, and R. M. Overney, *Direct measurement of nanofluxes and structural relaxations of perfluorinated ionomer membranes by scanning probe microscopy*, Journal of Membrane Science **279**, 608-14 (2006).
[45] J. P. Killgore, W. King, K. Kjoller, and R. M. Overney, *Heated-tip AFM: Applications in Nanocomposite Polymer Membranes and Energetic Materials*, Microscopy Today **15**, 20-5 (2007).